Molecule-Based Magnets Formed by Bimetallic Three-Dimensional Oxalate Networks and Chiral Tris(bipyridyl) Complex Cations. The Series $[Z^{II}(bpy)_3][ClO_4][M^{II}Cr^{III}(ox)_3]$ (Z^{II} = Ru, Fe, Co, and Ni; M^{II} = Mn, Fe, Co, Ni, Cu, and Zn; ox = Oxalate Dianion)

E. Coronado,* J. R. Galán-Mascarós,† C. J. Gómez-García, and J. M. Martínez-Agudo

Instituto de Ciencia Molecular, Universitat de Valencia, Dr. Moliner 50, E-46100 Burjasot, Spain

Received August 7, 2000

The synthesis, structure, and physical properties of the series of molecular magnets formulated as $[Z^{II}(bpy)_3][ClO_4][M^{II}Cr^{III}(ox)_3]$ (Z^{II} = Ru, Fe, Co, and Ni; M^{II} = Mn, Fe, Co, Ni, Cu, and Zn; ox = oxalate dianion) are presented. All the compounds are isostructural to the $[Ru(bpy)_3][ClO_4][MnCr(ox)_3]$ member whose structure (cubic space group $P4_132$ with $a = 15.506(2)$ Å, $Z = 4$) consists of a three-dimensional bimetallic network formed by alternating M^{II} and Cr^{III} ions connected by oxalate anions. The identical chirality (Λ in the solved crystal) of all the metallic centers determines the 3D chiral structure adopted by these compounds. The anionic 3D sublattice leaves some holes where the chiral $[Z(bpy)_3]^{2+}$ and ClO_4^- counterions are located. These compounds behave as soft ferromagnets with ordering temperatures up to 6.6 K and coercive fields up to 8 mT.

Introduction

It is well-known that extended networks of dimensionalities two and three can be constructed from oxalato-bridged bimetallic complexes.[1] In particular, bulky organic monocations stabilize two-dimensional structures[2] of formula $[XR_4][M^{II}M^{III}(ox)_3]$ (M^{II} = Mn, Fe, Co, Ni, Cu, Zn; M^{III} = Cr, Fe, Ru; X = N, P; R = *n*-alkyl, phenyl, ...) in which $[M^{III}(ox)_3]^{3-}$ are held together by the M^{II} cations in order to form negatively charged honeycomb layers interleaved by the organic cations which control the interlayer separation. These phases were first reported by Okawa et al.[3] in 1990, and the honeycomb structures were determined independently by Atovmyan et al.[4] and by Decurtins et al.[5] From the structural point of view the layers contain M^{II} and M^{III} tris(oxalate) sites of opposite configuration (Δ and Λ). The main interest of these 2D phases is related with their magnetic properties. These compounds behave as ferromagnets,[6] ferrimagnets[7] or canted antiferromagnets[8] with T_c ranging from 5 up to 44 K. An additional current interest of these phases comes from the possibility to substitute the "innocent" organic cations by electronically active cations able to add a second property to the solid while maintaining the layered structure in the search for new classes of molecule-based materials presenting association or coexistence of properties.[9,10]

A second type of bimetallic network is formed when the cations are chiral metallic complexes such as $[Z^{II}(bpy)_3]^{2+}$ (Z^{II} = Ru, Fe, Co, Ni, Zn). In that case a chiral three-dimensional structure is formed with general formula $[Z^{II}(bpy)_3][M^{I}M^{III}(ox)_3]$ or $[Z^{II}(bpy)_3][M^{II}M^{II}(ox)_3]$ (M^{II} = Mn, Fe, Co, Cu; M^{III} = Cr, Fe; M^{I} = alkali metal, NH_4^+). This 3D network was first reported by Decurtins et al.[11] in 1993. In contrast to the previous layered phases, in the 3D phase the two metal sites, M^{III} and M^{I}, have the same configuration (Δ or Λ). The network structure contains cavities wherein the $[Z^{II}(bpy)_3]^{2+}$ are located. These cavities have some flexibility and can also accommodate small monoanions X^- such as ClO_4^-, BF_4^-, or PF_6^-. This feature allows extending the range of compounds that can be obtained to the formulas $[Z^{III}(bpy)_3][X][M^{I}M^{III}(ox)_3]$ and $[Z^{III}(bpy)_3][X][M^{II}M^{II}(ox)_3]$ (Z^{III} = Cr, Rh).[12] From the magnetic point of view, the 3D oxalate networks reported to date are less interesting than the 2D phases since only the homometallic series $[M^{II}M^{II}]$ lead to ordered magnetic phases (antiferromagnets or weak ferromagnets).[13] In the bimetallic series $[M^{I}M^{III}]$, the magnetic M^{III} centers are surrounded by diamagnetic alkali ions, M^{I}, so that they behave as simple paramagnets. Still, interesting photophysical properties have been described for these paramagnetic compounds due to the presence of two transition metal ions (as Ru^{II} and Cr^{III}) which can give rise to photoinduced

* Corresponding author. E-mail: eugenio.coronado@uv.es.
† Present address: Department of Chemistry, Texas A&M University, College Station, TX 77843.

(1) Decurtins, S.; Pellaux, R.; Hauser, A.; Von Arx, M. E. In *Magnetism: A Supramolecular Function*; Kahn, O., Ed.; NATO-ASI Series C484; Kluwer Academic Press: New York, 1996; p 487.
(2) Pellaux, R.; Schmalle, H. W.; Huber, R.; Fisher, P.; Hauss, T.; Ouladdiaf, B.; Decurtins, S. *Inorg. Chem.* **1997**, *36*, 2301.
(3) (a) Zhong, Z. J.; Matsumoto, N.; Okawa, H.; Kida, S. *Chem. Lett.* **1990**, 87. (b) Ohba, M.; Tamaki, H.; Matsumoto, N.; Okawa, H.; Kida, S. *Chem. Lett.* **1991**, 1157.
(4) Atovmyan, L. O.; Shilov, G. V.; Lyubovskaya, R. N.; Zhilyaeva, E. I.; Ovanesyan, N. S.; Pirumova, S. I.; Gusakovskaya, I. G. *JETP Lett.* **1993**, *58*, 766.
(5) (a) Decurtins, S.; Schmalle, H. W.; Oswald, H. R.; Linden, A.; Ensling, J.; Gütlich, P.; Hauser, A. *Inorg. Chim. Acta* **1994**, *216*, 65. (b) Pellaux, R.; Schmalle, H. W.; Huber, R.; Fisher, P.; Hauss, T.; Ouladdiaf, B.; Decurtins, S. *Inorg. Chem.* **1997**, *36*, 2301.
(6) Tamaki, H.; Zhong, Z. J.; Matsumoto, N.; Kida, S.; Koikawa, M.; Achiwa, N.; Hashimoto, Y.; Okawa, H. *J. Am. Chem. Soc.* **1992**, *114*, 6974.
(7) Tamaki, H.; Mitsumi, M.; Nakamura, K.; Matsumoto, N.; Kida, S.; Okawa, H.; Iijima, S.; *Chem. Lett.* **1992**, 1975.
(8) Mathonière, C.; Nuttall, J.; Carling, S. G.; Day, P. *Inorg. Chem.* **1996**, *35*, 1201.
(9) (a) Clemente-León, M.; Coronado, E.; Galán-Mascarós, J. R.; Gómez-García, C. J. *Chem. Commun.* **1997**, 1727. (b) Coronado, E.; Galán-Mascarós, J. R.; Gómez-García, C. J. *Synth. Met.* **1999**, *102*, 1450.
(10) Gu, Z.; Sato, O.; Iyoda, T.; Hashimoto, K.; Fujishima, A. *Mol. Cryst. Liq. Cryst.* **1996**, *286*, 147.
(11) Decurtins, S.; Schmalle, H. W.; Schneuwly, P.; Oswald, H. R. *Inorg. Chem.* **1993**, *32*, 1888.
(12) Decurtins, S.; Schmalle, H. W.; Pellaux, R.; Schneuwly, P.; Hauser, A. *Inorg. Chem.* **1996**, *35*, 1451.
(13) Hernández-Molina, M.; Lloret, F.; Ruiz-Pérez, C.; Julve, M. *Inorg. Chem.* **1998**, *37*, 4131.

10.1021/ic0008870 CCC: $20.00
Published on Web 12/02/2000

processes such as energy transfer or electron transfer.[12,14] In one case, namely $[Co(bpy)_3][LiCr(ox)_3]$, a thermal spin transition for the Co^{II} complex has recently been observed.[15]

The best way to obtain magnets in these 3D phases is by constructing a $[M^{II}M^{III}]$ bimetallic network analogous to the bimetallic layered magnets cited above. Although this possibility has been postulated several times since the discovery of the 3D oxalate network, the preparation of these phases has not been reported to date. That is probably due to the difficulty of obtaining a pure $[M^{II}M^{III}]$ bimetallic network as M^{I} ions can also enter in the structure. Here we report the synthesis, structures, and magnetic characterization of this new series of bimetallic magnets of general formula $[Z^{II}(bpy)_3][ClO_4][M^{II}Cr^{III}(ox)_3]$ (Z^{II} = Ru, Fe, Co, Ni; M^{II} = Mn, Fe, Co, Ni, Cu, Zn). These compounds will be abbreviated as [Z/MCr].

Experimental Section

Materials. The complexes $[Z^{II}(bpy)_3]^{2+}$ (Z^{II} = Ru, Fe, Co, Ni) were prepared according to the literature methods.[16] The precursor salt $Ag_3[Cr(ox)_3]\cdot nH_2O$ was prepared by methatesis from the corresponding potassium salt.[17]

General Synthetic Procedure for $[Z(bpy)_3][ClO_4][MCr(ox)_3]$. An excess of $MCl_2\cdot 4H_2O$ (4 mmol) was added to a suspension of $Ag_3[Cr(ox)_3]\cdot nH_2O$ (0.3 g; 0.5 mmol) in methanol (20 mL). The AgCl precipitate immediately formed was filtered, and then the clear solution was added dropwise to a methanol solution (50 mL) of $[Z(bpy)_3]Cl_2$ or $[Z(bpy)_3][ClO_4]_2$ (0.5 mmol) and $M[ClO_4]_2\cdot nH_2O$ (2 mmol). After $^1/_2$ h a fine bright powder was filtered off and washed with methanol, DMF, water, and acetone and dried at room temperature. The composition of all samples was checked by microanalysis, indicating the complete absence of K^+ and the expected ratio among metals.

Single crystals of $[Ru(bpy)_3][ClO_4][MnCr(ox)_3]$ of good quality for X-ray diffraction analysis were obtained by an analogous procedure by slow diffusion of both solutions in a H-tube after 3 months.

Structural Determination. Good-quality single crystals of $[Ru(bpy)_3][ClO_4][MnCr(ox)_3]$ were collected, and one of them was mounted on a CAD4 Enraf-Nonius X-ray diffractometer. Unit cell parameters and orientation matrix were determined by least-squares fit of 25 independent reflections. Data collection was performed with the ω-scan technique with three standard reflections measured every 2 h which showed no significant decay. Lorentz, polarization, and empiric absorption (ψ scan) corrections were carried out. The structure was solved by direct methods using the SIR97 program,[18] and was refined on F^2 using the SHELXL-97 program.[19] In the structural determination the heavy atoms from anionic and cationic species were found immediately, and the other atoms were located through successive Fourier differences. The perchlorate anions were found to be disordered. The chlorine is located on an inversion center, and significant electronic density was found around this position at very near distances, which suggests that the perchlorate anion can adopt slightly different random positions due to its small size compared to the hole left by the structure. In addition, the possibility of free rotation and the presence of the inversion center changes the expected tetrahedral configuration to a more complicated configuration with at least eight oxygen positions surrounding the chlorine, with occupancy factors less than 1. Thus, to handle these disorder problems, the best models were found to be those with two crystallographically independent oxygen positions from the perchlorate anions. All atoms were refined anisotropically except hydrogens and the oxygen atoms from the perchlorate units.

Table 1. Crystal Data and Structure Refinement Data for $[Ru(bpy)_3][ClO_4][MnCr(ox)_3]$

formula	$C_{36}H_{24}ClCrMnN_6O_{16}Ru$
a (Å)	15.506(2)
V (Å$^{3)}$	3728(2)
Z	4
F_w	1040.10
space group	$P4_132$
T (K)	293(2)
λ (Å)	0.71069
ρ_{calc} (g cm^{-3})	1.853
μ (cm^{-1})	1.179
$R_1{}^a$	0.0263
$R_2{}^b$	0.0642

^{a} $R_1 = \sum(F_o - F_c)/\sum(F_o)$. ^{b} $R_2 = [\sum[\omega(F_o^2 - F_c^2)^2]/\sum[\omega(F_o^2)^2]]^{1/2}$; $\omega = 1/[\sigma^2(F_o^2) + (0.1446P)^2 + 4.8035P]$, where $P = (F_o^2 + 2F_c^2)/3$.

Crystallographic data and refinement parameters are summarized in Table 1. Atomic coordinates, anisotropic thermal parameters, the labeling scheme, bond distances, and bond angles are provided as Supporting Information.

Magnetic Properties. Variable-temperature susceptibility measurements were carried out on polycrystalline samples with a magnetometer (Quantum Design MPMS-XL-5) equipped with a SQUID sensor. The dc measurements were performed in the temperature range 2−300 K at a magnetic field of 0.1 T. The ac measurements were performed in the temperature range 2−20 K at different frequencies with an oscillating magnetic field of 0.395 mT. The magnetization and hysteresis studies were performed between 5 and −5 T, cooling the samples at zero field.

Results and Discussion

Synthesis and Structure. The main synthetic problem to be overcome in order to prepare the oxalate-based 3D $[M^{II}M^{III}(ox)_3]$ phases is to avoid the formation of the analogous $[M^{I}M^{III}(ox)_3]$ phases. Our first attempts at preparing these salts were unsuccessful since the presence of alkali metal ions or NH_4^+ in solution (coming for instance from the tris(oxalato)metalate salt, which is a common starting material for the synthesis of the bimetallic systems) yielded impure compounds. In these cases the monocations were found to randomly occupy the corresponding M^{II} position in the network, promoting at the same time the absence of the charge-compensating anion (usually ClO_4^-). Of course, bulky organic cations also caused problems since their presence in solution templated the formation of the 2D phases. Thus, the synthetic procedures were designed to completely avoid the presence of any cations in solution other than the transition metal species. For the Cr^{III} derivatives, $Ag_3[Cr^{III}(ox)_3]$ is used as the source for $[Cr^{III}(ox)_3]^{3-}$. Reaction of this silver salt with excess of the chloride salt of the divalent metal gave insoluble AgCl that was removed by filtration, and a solution that only contained as metals the desired divalent cation, M^{II}, and the $[Cr^{III}(ox)_3]^{3-}$ complex. By addition of the corresponding tris(bipyridyl) complex $[Z^{II}(bpy)_3]^{2+}$, and using as perchlorate source the salt of the desired divalent metal (and also the $[Z^{II}(bpy)_3]$ salt in some cases), the desired 3D compounds were obtained as very fine polycrystalline precipitates after several minutes. Particle sizes are typically uniform and of the order 0.5−3 μm, except for the $[Ru(bpy)_3][ClO_4][NiRu(ox)_3]$ derivative, which presents uniform particle sizes of less than 0.2 μm. Unfortunately, the same synthetic approach could not be used for the Fe^{III} derivatives, since the $Ag_3[Fe^{III}(ox)_3]$ salt is not stable.

(14) Hauser, A.; Riesen, H.; Pellaux, R.; Decurtins, S. *Chem. Phys. Lett.* **1996**, *261*, 313.
(15) Sieber, R.; Decurtins, S.; Stoeckli-Evans, H.; Wilson, C.; Yufit, D.; Howard, J. A. K.; Capelli, S. C.; Hauser, A. *Chem. Eur. J.* **2000**, *6*, 361.
(16) (a) Burstall, F. H.; Nyholm, R. S. *J. Chem. Soc.* **1952**, 3570. (b) Anderson, S.; Seddon, K. R. *J. Chem. Res.* **1979**, 74.
(17) Baylar, J. C.; Jones E. M. In *Inorganic Synthesis*; Booth, H. S., Ed.; McGraw-Hill: New York, 1939; Vol. 1, p 35.
(18) Altomare, A.; Burla, M. C.; Camalli, M.; Cascarano, G.; Giacovazzo, C.; Guagliardi, A.; Moliterni, A. G. G.; Polidori, G.; Spagna, R. *J. Appl. Crystallogr.* **1999**, *32*, 115.
(19) Sheldrick, G. M. University of Göttingen, Germany, 1997.

Table 2. Unit Cell Parameters for the Series $[Z(bpy)_3][ClO_4][MCr(ox)_3]$

[Z/M]	*a* (Å)	*V* (Å^3)
[Ru/Mn][a]	15.506(2)	3728(3)
[Ru/Fe]	15.46(3)	3695(43)
[Ru/Co]	15.51(4)	3731(58)
[Ru/Ni]	15.40(8)	3652(114)
[Ru/Cu]	15.41(7)	3659(107)
[Fe/Mn]	15.43(4)	3673(57)
[Fe/Fe]	15.30(5)	3581(70)
[Fe/Co]	15.38(6)	3638(85)
[Ni/Mn]	15.45(4)	3688(57)
[Ni/Fe]	15.44(6)	3680(86)
[Co/Mn]	15.49(5)	3716(72)

[a] Single-crystal data.

Not all possible Z/M^{II} combinations could be obtained. In some cases, as with M^{II} = Ni and Cu, no solid precipitate appeared in the reaction solution. This is not unusual since, for instance, the analogous Ni^{II} 2D derivatives have not been reported. This should be related to the smaller size of Ni and Cu compared to the rest of the divalent first-row transition metals. Only with $[Ru(bpy)_3]^{2+}$ (the biggest cation used) were these derivatives obtained. In other cases, a precipitate is formed but not with the expected composition due to the poor stability of the starting $[Z^{II}(bpy)_3]^{2+}$ complexes in solution in the presence of other divalent metals. Thus, the synthesis aiming the [Co/FeCr] derivative yielded [Fe/FeCr] instead, because of the larger stability of the $[Fe(bpy)_3]^{2+}$ complex: $[Co(bpy)_3]^{2+}$ in the presence of free Fe^{2+} gives $[Fe(bpy)_3]^{2+}$ and free Co^{2+}. As a result, the final compound does not include any Co, not even in the bimetallic network.

By slow diffusion, crystals of good enough quality for X-ray diffraction analysis were grown for the salt $[Ru(bpy)_3][ClO_4][MnCr(ox)_3]$. All other [Z/MCr] compounds reported in this work were obtained as polycrystalline materials that were found to be isostructural by X-ray powder diffraction. The cell parameters derived from the powder diffractograms are summarized in Table 2. These compounds crystallize in the cubic space group $P4_132$, as their analogues $[M(bpy)_3][ClO_4][M_2(ox)_3]$, and present the expected well-known 3D 3-connected 10-gon oxalate-based anionic network (10,3).[11,20] This network is formed by bis-bidentate oxalate ligands connecting M^{II} and M^{III} metal ions in such a way that each M^{II} ion is surrounded by three Cr^{III} ions and vice versa, leading to polymeric nets with all the metal ions maintaining the same chirality. Both metals are equivalent by X-ray analysis. Otherwise, the space group would have been $P2_13$, as found in the $[Z(bpy)_3][ClO_4][M^IM^{III}(ox)_3]$ analogues (M^I = alkali metal), where both metal sites are nonequivalent.[20] Therefore, in the [Ru/MnCr] compound Mn and Cr occupy the same crystallographic position, with mean M−O distances of 2.098 and 2.109 Å; these distances are comprised between the shorter ones expected for Cr^{III}−O and the longer ones expected for Mn^{II}−O. These loosely otherwise networks are stabilized by the $[Ru(bpy)_3]^{2+}$ cations of the appropriate chirality located in the vacancies of the polymeric anionic framework. Projections of the anionic host and the cationic guest are shown in Figure 1. Perchlorate anions needed for electroneutrality fill the holes left by the cation complexes. In our case, the crystal structure that has been solved corresponds to the Λ chirality.

Magnetic Properties. *Salts Based upon $[Ru(bpy)_3]^{2+}$ Complexes.* Derivatives of this diamagnetic cation with M^{II} = Mn, Fe, Co, Ni, and Cu have been studied. The magnetic susceptibility behaviors of all these compounds are essentially similar. All members obey the Curie−Weiss law from 50 to 300 K. The resulting parameters are summarized in Table 3. The derived Curie constants of the compounds are within the values expected for the sum of Curie constants of the constituent metal ions (Table 3). In all compounds the Weiss constants, Θ, are positive,

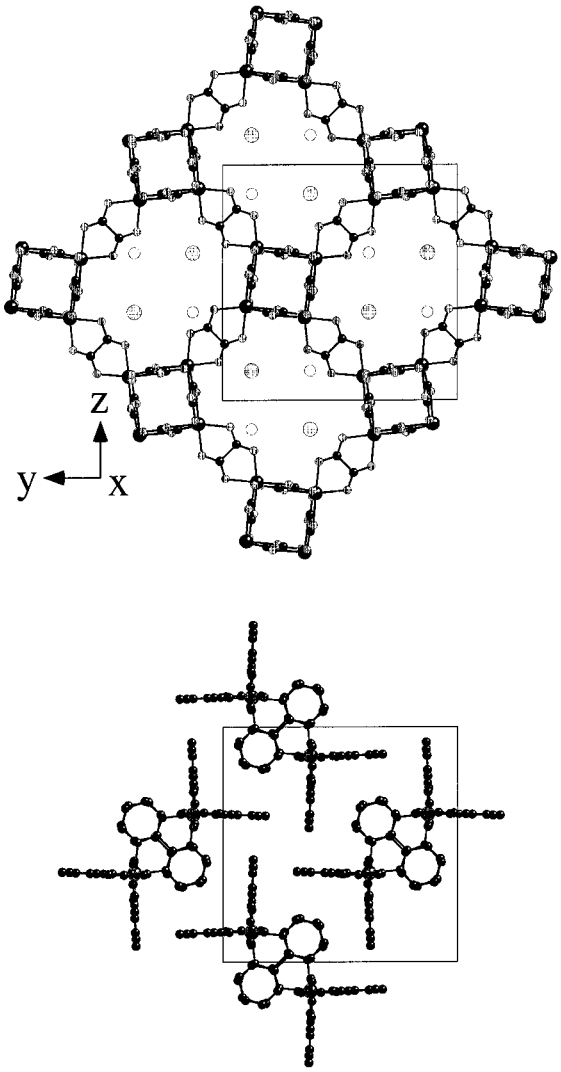

Figure 1. (top) Projection in the *bc* plane of the structure of the family of molecule-based magnets $[Z(bpy)_3][ClO_4][MCr(ox)_3]$. Only the Z^{II} ion (in gray) of $[Z(bpy)_3]^{2+}$ cations and the Cl atom (in white) of the ClO_4^- anions are drawn in the cavities. (bottom) Projection of the $[Z(bpy)_3]^{2+}$ cations in the same structure.

Table 3. Magnetic Parameters for the Series $[Z(bpy)_3][ClO_4][MCr(ox)_3]$[a]

Z(II)	M(II)	T_c (K)	θ (K)	*C* (emu·K·mol^{-1})	*M* (μ_B) at 5 T	theor M_s (μ_B)	H_{coer} (mT)
Ru	Mn	<2.0	5.0	5.9	6.7	8	0
	Fe	2.5	9.0	4.9	5.0	7	1.4
	Co	2.8	6.9	4.7	4.9	6	0.8
	Ni	6.4	16.9	3.0	4.0	5	2.2
	Cu	1.9	9.4	2.5	3.9	4	1.4
Fe	Mn	3.9	4.2	6.2	6.0	8	0
	Fe	4.7	2.0	5.2	4.5	7	8.0
	Co	6.6	1.1	5.1	5.0	6	5.5
Ni	Mn	2.3	2.6	6.6	7.7	10	1.3
	Fe	4.0	2.2	5.8	5.8	9	2.8
Co	Mn	2.2	1.1	7.4	7.5	11	1.3

[a] *M* and H_{coer} are values at 2 K.

(20) Decurtins, S.; Schmalle, H. W.; Schneuwly, P.; Ensling, J.; Gütlich, P. *J. Am. Chem. Soc.* **1994**, *116*, 9521.

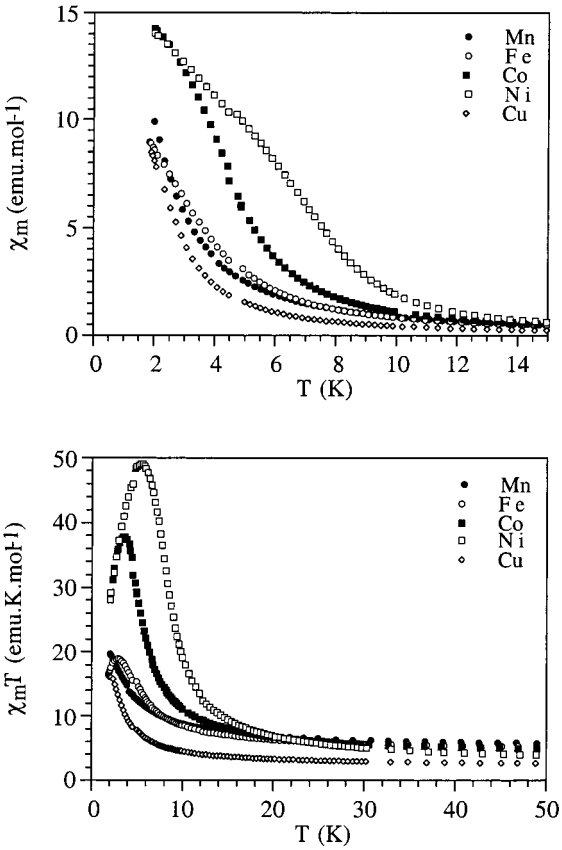

Figure 2. (top) Thermal variation of the magnetic susceptibility at 0.1 T (χ_m) for the Ru/MCr series. (bottom) Thermal variation of the product of the magnetic susceptibility times the temperature ($\chi_m T$) for the same family.

indicating ferromagnetic interactions between neighboring Cr^{III} and M^{II} ions. This is also supported by the gradual increase observed in the χT product upon cooling from room temperature. At low temperatures (below 10 K) both χ and χT show sharp increases; in some cases, a tendency to saturation in χ is also observed upon cooling (Figure 2). These features suggest the onset of long-range ferromagnetic ordering. To confirm the appearance of magnetic ordering and to precisely determine the critical temperatures, ac susceptibility measurements were performed. Typically, in a magnet containing net magnetic moments in the ordered state (ferromagnet, ferrimagnet, or canted antiferromagnet, for example) these measurements show a maximum in the in-phase signal (χ') near T_c and an out-of-phase signal (χ'') that starts to appear at temperatures just below T_c. Therefore, the position of this signal provides a precise way to determine T_c. In the derivatives of Mn, Fe, and Cu χ' shows a continuous increase with no maximum down to 1.8 K, indicating that in these three cases the magnetic ordering may occur near or below this temperature (Figure 3, top and center). This point is confirmed by the out-of-phase signals. In the Mn derivative a very weak rise in χ'' is observed near 2 K, which indicates that the magnetic ordering is probably close to this temperature. As crystals of this sample can also be prepared, we have compared the behavior of the powder with that of the crystals. No significant differences have been detected. In Fe and Cu derivatives sharp increases in χ'' are seen at 2.5 and 1.9 K, respectively (Figure 3, top). These results provide an accurate determination of T_c in the two latter compounds. On the other hand, in the Co and Ni derivatives, a maximum in χ' is clearly observed at 2.4 and 6.1 K, respectively, together with the corresponding χ'' signals (Figure 3, bottom). From these signals,

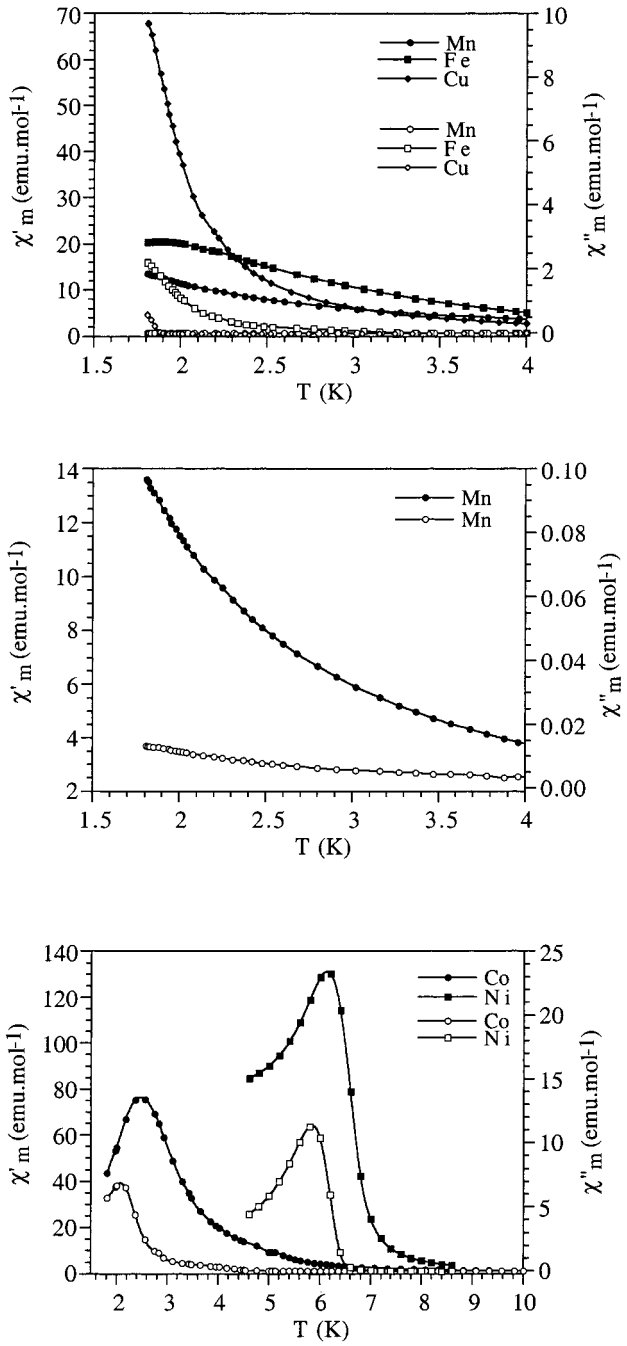

Figure 3. Thermal variation of the in-phase (filled symbols, χ_m') and out-of-phase (empty symbols, χ_m'') ac susceptibility of the Mn, Fe, and Cu derivatives (top), the Mn derivative (center), and the Co and Ni derivatives (bottom) of the Ru/MCr series.

the estimated T_c values are 2.8 and 6.4 K, respectively. Notice that in all the above compounds the maxima in χ' and χ'' are practically frequency independent. For example, in the Ni derivative the maxima in χ' and χ'' only vary around 0.2 K when the frequency is varied a factor of more than 300 (from 1 to 332 Hz, Figure 4, top). This weak variation may be related to the small particle size of the sample in this case. A more pronounced variation is, however, observed in the Fe derivative, which shows a maximum in χ' which is shifted from less than 1.8 to 2.1 K when the frequency increases a factor of approximately 100 (from 10 to 997 Hz, Figure 4, bottom). Similar behaviors have already been observed in the related 2D phases and have been attributed to the presence of small amounts of Fe^{III} ions in the bimetallic network that introduces some

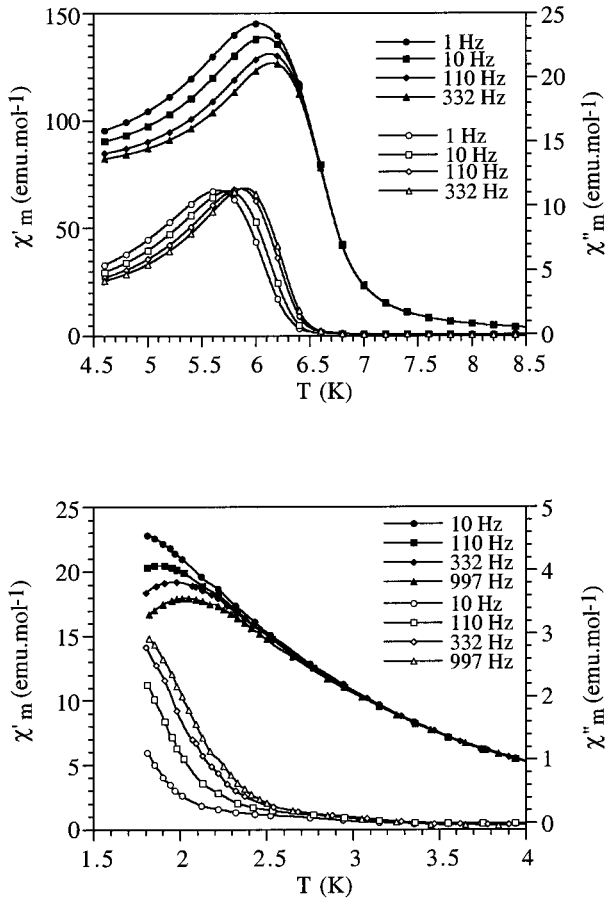

Figure 4. Frequency dependence of the in-phase (filled symbols, χ_m') and out-of-phase (empty symbols, χ_m'') ac susceptibility of the Ru/NiCr (top) and Ru/FeCr (bottom) derivatives.

additional magnetic disorder in the lattice as a result of the presence of antiferromagnetic $Fe^{III}-Fe^{II}$ interactions competing with $Cr^{III}-Fe^{II}$ interactions.[21]

The nature of the above magnetic transitions corresponds to a ferromagnetic ordering as demonstrated by the field dependence of the isothermal magnetization performed at 2 K (1.9 K in the Cu derivative). In fact, one observes a rapid increase of the magnetization with H which is much faster than the rise expected for noninteracting Cr^{III} and M^{II} ions (dotted lines in Figure 5). The *M* values at 5 T are compatible with a parallel alignment of the interacting spins (Figure 5, top; Table 3). This sharp increase is more gradual in those compounds having T_c values close to 2 K (Mn, Fe, and Cu; Figure 5, bottom). Notice that the magnetic field required to approach the saturation is rather large in all cases. Furthermore, no clear saturation of the magnetization is observed in any case and the *M* values at 5 T are smaller than the sum of the spin values of the two magnetic sublattices (see the theoretical M_s values in Table 3). These features have already been noted in the analogous 2D series and have been attributed to the presence of a spin canting in the ferromagnetic structure. Below T_c, the magnetic hysteresis loops of these compounds show coercive fields close to zero, which indicate that these compounds can be referred to as very soft ferromagnets. The largest coercive field is observed in the Ni derivative (2.2 mT) (Table 3).

Salts Based upon Other $[Z(bpy)_3]^{2+}$ Complexes (Z^{II} = Fe, Co, Ni). To study the influence of the $[Z(bpy)_3]^{2+}$ cation on

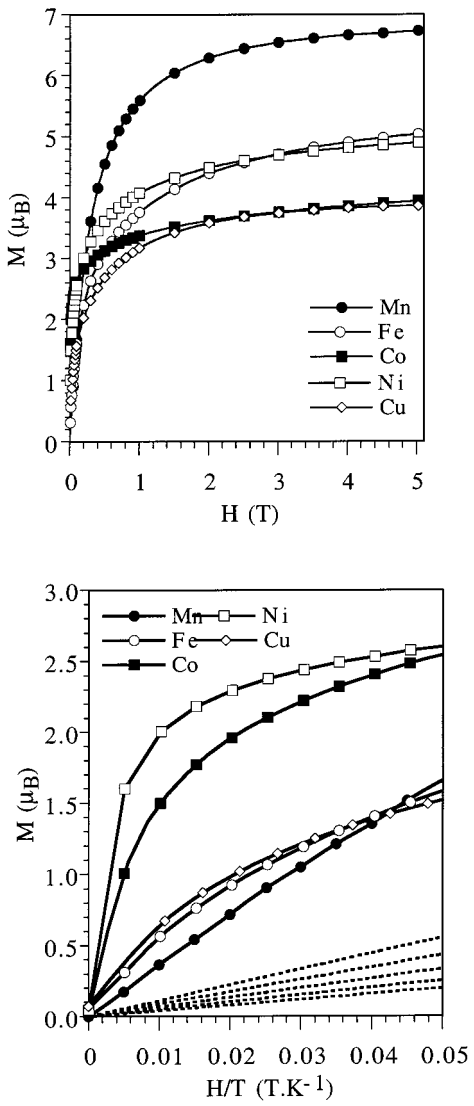

Figure 5. (top) Isothermal magnetization at 2 K of the Ru/MCr series. (bottom) The low field region. The dotted lines are the expected behaviors for non interacting Cr^{III} and M^{II} ions (M^{II} = Mn, Fe, Co, Ni, and Cu, from top to bottom, respectively).

the magnetic properties of the salts, we report here the magnetic properties of the salts formed by the ferromagnetic 3D networks [MnCr], [FeCr], and [CoCr] with the diamagnetic cation $[Fe(bpy)_3]^{2+}$ ([Fe/MnCr], [Fe/FeCr], and [Fe/CoCr]). We also report the properties of the salts containing the paramagnetic cations $[Ni(bpy)_3]^{2+}$ ([Ni/MnCr] and [Ni/FeCr]) and $[Co(bpy)_3]^{2+}$ ([Co/MnCr]). In general, the magnetic features of all these compounds closely resemble those reported for the analogous $[Ru(bpy)_3]^{2+}$ derivatives (see Table 3). Thus, most of the compounds obey the Curie−Weiss law. The only exceptions are the Co-containing compounds [Fe/CoCr] and [Co/MnCr] wherein a small and negative Weiss constant is calculated. Such a difference is not due to a different sign of the exchange interaction in these compounds but to the orbital degeneracy of the high-spin Co(II) ion in an octahedral environment since its effect on the magnetic moment can overcome the positive contribution to Θ coming from the weak ferromagnetic coupling. Furthermore, all are very soft ferromagnets as demonstrated by the magnetization measurements and hysteretic behaviors (Figure 6; Table 3). Thus, in these three series the field dependence of the isothermal magnetization performed at 2 K shows a behavior similar to that observed in the $[Ru(bpy)_3]^{2+}$ derivatives: a rapid

(21) Coronado, E.; Galán-Mascarós, J. R.; Gómez-García, C. J.; Ensling, J.; Gütlich, P. *Chem. Eur. J.* **2000**, *6*, 552.

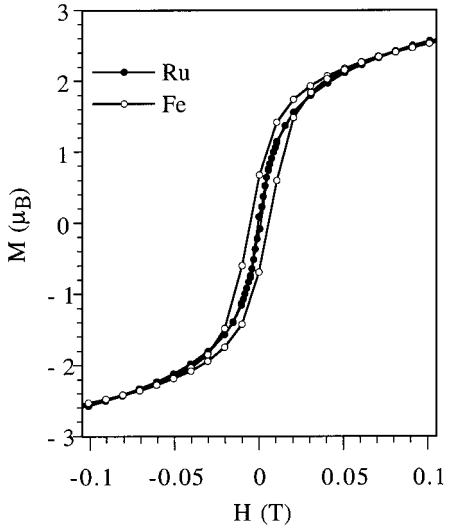

Figure 6. Hysteresis cycle at 2 K of the Z/CoCr series.

raise of the magnetization with *H*, although without a clear saturation of the magnetization even at 5 T, where a value close to that expected for a parallel alignment of the interacting spins is reached (Figure 7; Table 3). As in the analogous 2D series and in the $[Ru(bpy)_3]^{2+}$ series, the differences with the theoretical values can be attributed to the presence of a spin canting in the ferromagnetic structure.

Finally, when the cationic complex is paramagnetic, the magnetization measurements and the Curie constants are approximately the sum of the magnetic contributions coming from the two kinds of magnetic sublattices. This observation indicates that the two magnetic sublattices essentially behave independently. Still, significant variations in both the critical temperatures and the coercive fields are observed. Thus, in the [MnCr] series a significant increase from $T_c \leq 2$ K in the $[Ru(bpy)_3]^{2+}$ complex to 3.9 K in the $[Fe(bpy)_3]^{2+}$ complex is observed (Figure 8, top). A similar variation is observed in the [FeCr] and [CoCr] series wherein T_c increases, respectively, from 2.5 and 2.8 K in the $[Ru(bpy)_3]^{2+}$ derivatives to 4.7 and 6.6 K in the $[Fe(bpy)_3]^{2+}$ derivatives (Figure 8, center and bottom). As a general rule, we observe that the magnets containing the $[Ru(bpy)_3]^{2+}$ complex, which is the biggest one, exhibit the lowest T_c values, while those containing $[Fe(bpy)_3]^{2+}$ exhibit the highest values. The magnetic Ni(II) and Co(II) tris(bpy) complexes show intermediate values. From this tendency it is apparent that the observed variation depends on the size of the inserted complex, whereas the electronic nature (magnetic or not) of the metal is not a relevant factor.

The increase in the critical temperatures of the $[Fe(bpy)_3]^{2+}$ derivatives with respect to the $[Ru(bpy)_3]^{2+}$ ones allows determination in a more accurate way the values of T_c, since sharp out-of-phase signals are clearly observed in the ac magnetic measurements well above the lowest available temperature. Furthermore, this feature also allows better characterization of the weak but detectable frequency dependence found in the [FeCr] series, since the range of frequencies wherein the maxima in χ' and χ'' are observed can now be expanded. For example, in the [Fe/FeCr] compound we observe that the maximum in χ' is shifted from 3.5 to 3.8 K when the frequency varies from 1 to 332 Hz, and the same holds for the maximum in χ'' which shifts from 3.1 to 3.5 K (Figure 9).

Conclusions

In this paper we have shown that the three-dimensional chiral

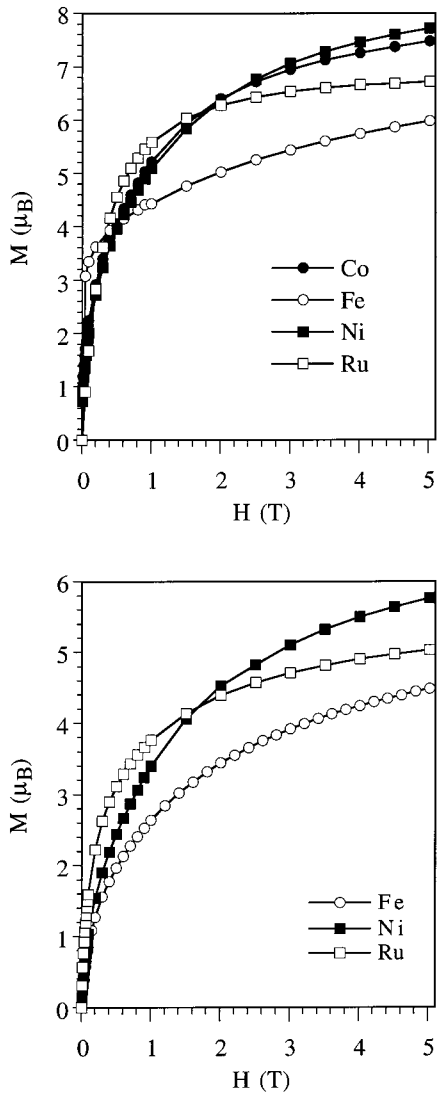

Figure 7. Isothermal magnetization at 2 K of the Z/MnCr (top) and Z/FeCr (bottom) series.

structure adopted by the bimetallic oxalato complexes when they react with $[Z^{II}(bpy)_3]^{2+}$ complexes (Z^{II} = Ru, Fe, Co, Ni) can be used to build up an extensive series of molecule-based ferromagnets formulated as $[Z^{II}(bpy)_3][ClO_4][M^{II}Cr^{III}(ox)_3]$ (M^{II} = Mn, Fe, Co, Ni, Cu, Zn). Eleven members of this novel series have been obtained and their magnetic properties investigated in this work.

When compared with the phases of two-dimensional layered magnets based upon bimetallic oxalato complexes, this series shows several distinctive features worthwhile to mention:

(i) The influence of the molecular cationic network on the magnetic properties is much stronger in the 3D series than in the analogous 2D series. Thus, in the 2D series it has been found that insertion of organic and organometallic cations of various sizes, shapes, and symmetries has little influence on the critical temperatures of the magnet. On the contrary, in the 3D series reported here the inserted cation strongly affects the T_c values. A similar effect has been observed in the 3D related families $[Co^{III}(bpy)_3][Co_2(ox)_3](ClO_4)$ and $[Z^{II}(bpy)_3][Co_2(ox)_3]$ (Z^{II} = Fe and Ni) where the increase in the cationic volume produces a decrease (and even a disappearance in the Ni case) in the ordering temperature to a spin canted ferromagnetic state.[13] A possible reason for this cationic effect on T_c is that the 3D network is less rigid than the planar 2D network. This flexibility

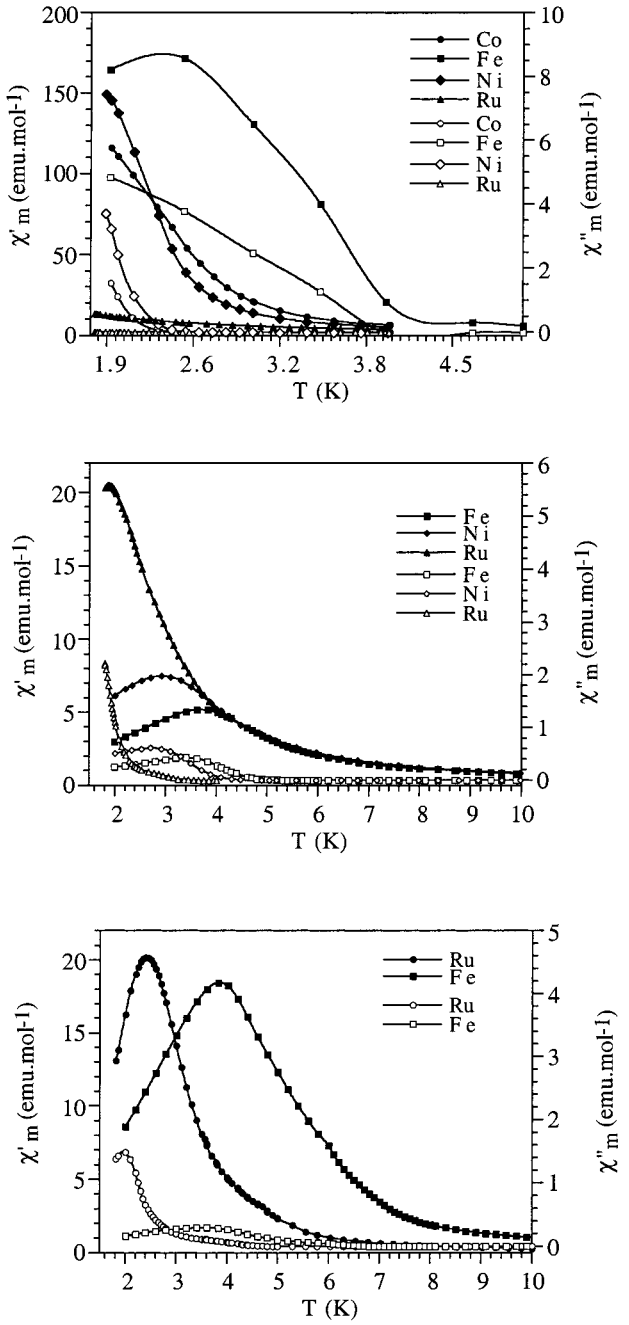

Figure 8. Thermal variation of the in-phase (filled symbols, χ_m') and out-of-phase (empty symbols, χ_m'') ac susceptibility for the series Z/MnCr (top), Z/FeCr (center), and Z/CoCr (bottom).

of the 3D network is shown by its ability to host one or two ions in the holes present in the structure ($[Z^{II}(bpy)_3]^{2+}$ and $(ClO_4)^-$ in the examples reported here, but other compensating ions as the $(BF_4)^-$ can also be inserted). This feature will directly affect the intermetallic bond angles and distances and, therefore, the exchange interactions within the $M^{II}Cr^{III}$ network. In the 2D structure these exchange interactions are not affected by the inserted cation that determines the interlayer separation but not the structural features within the $M^{II}Cr^{III}$ layer.

(ii) In all cases the critical temperatures of the 3D series are lower than those of the 2D phases (Table 4). Apparently this is a surprising result since a dramatic increase in T_c can be anticipated when the dimensionality of a system increases from 2 to 3, while keeping the exchange interactions unchanged. However, if we look at the connectivity between the exchange-coupled metal centers, we observe that in both cases each metal is surrounded by three nearest neighbors. Therefore, although the dimensionality changes, the connectivity remains 3 in both networks and the reason for this decrease is rather related with a weakening of the exchange interactions. The 2D network is planar, and it is easy to see how in this structure the C_3 axes of adjacent distorted octahedra remain parallel to each other. On the other hand, the nonplanarity of the 3D network forces the C_3 axes of adjacent octahedra to be perpendicular to each other (Figure 10). This different disposition should be responsible for the different exchange interaction found in these two phases, and shows that the exchange interactions through the oxalato bridge are optimized in the 2D network.

(iii) These 3D magnets are chiral. In each single crystal all metallic centers present the same configuration (Δ or Λ). Although a polycrystalline sample would be formed by a racemic mixture of Δ and Λ crystals, studies on the interplay between chirality and ferromagnetism can be performed on

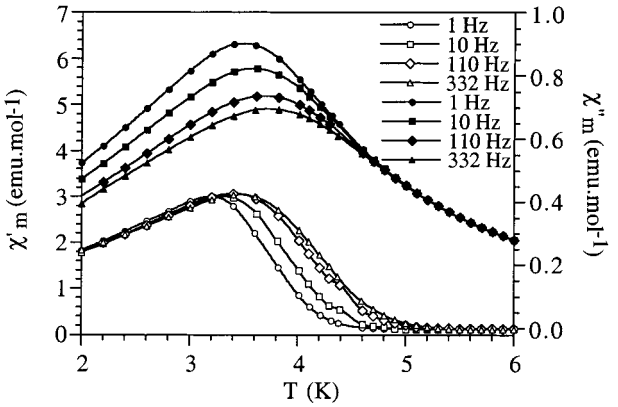

Figure 9. Frequency dependence of the in-phase (filled symbols, χ_m') and out-of-phase (empty symbols, χ_m'') AC susceptibility of the Fe/FeCr derivative.

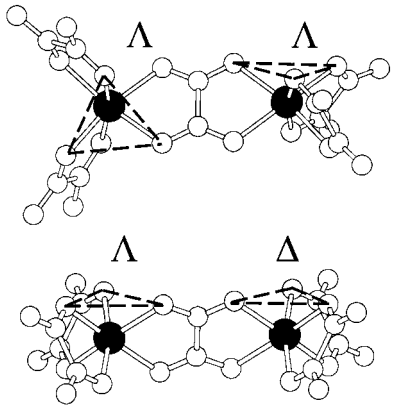

Figure 10. The MCr unit when the $M(ox)_3$ and $Cr(ox)_3$ complexes have the same chirality, giving rise to the 3D family (top), or different chirality, giving rise to the 2D family (bottom).

Table 4. Magnetic Parameters for the 2D Series [A][$MCr(ox)_3$] (A = $[NBu_4]^+$, $[CoCp^*_2]^+$, $[FeCp^*_2]^+$ [21])

	$[CoCp^*_2]^+$		$[FeCp^*_2]^+$		$[NBu_4]^+$	
M^{II}	T_c (K)	H_{coer} (mT)	T_c (K)	H_{coer} (mT)	T_c (K)	H_{coer} (mT)
Mn	5.1	4.0	5.3	2.0	6	2.0
Fe	12.7	194.0	13.0	110.0	12	32.0
Co	8.2	25.0	9.0	13.0	10	8.0
Cu	6.7	20.0	7.0	18.0	7	3.0

single crystals. Such materials are likely candidates to show a significant magneto-chiral effect.[22]

(iv) Finally, it is worthwhile to mention that the magnetic measurements for the $[Co^{II}(bpy)_3]^{2+}$ derivative indicate that this ion stays down to 2 K in the high-spin configuration and does not undergo any spin transition. This is in full agreement with the lattice parameters of these two salts that closely resemble that of the NaCr network, bigger than that of the LiCr network, where spin transition has been observed.[15]

(22) Rikken, G. L. J. A.; Raupach, E. *Nature* **1997**, *390*, 493.

Acknowledgment. This work was supported by the Spanish Ministerio de Ciencia y Tecnología (MCT) (Grants MAT98/0880 and 1FD97-1765) and the European Union (Network ERBFMRXCT 980181 on Molecular Magnetism: From Materials Toward Devices).

Supporting Information Available: Listings of the crystallographic and refinement data, atomic coordinates, thermal parameters, bond distances and angles and labeling schemes for the Ru/MnCr derivative. This material is available free of charge via the Internet at http://pubs.acs.org.

IC0008870